Electronic Supplementary Material (ESI) for Journal of Materials Chemistry A.


# Supporting Information

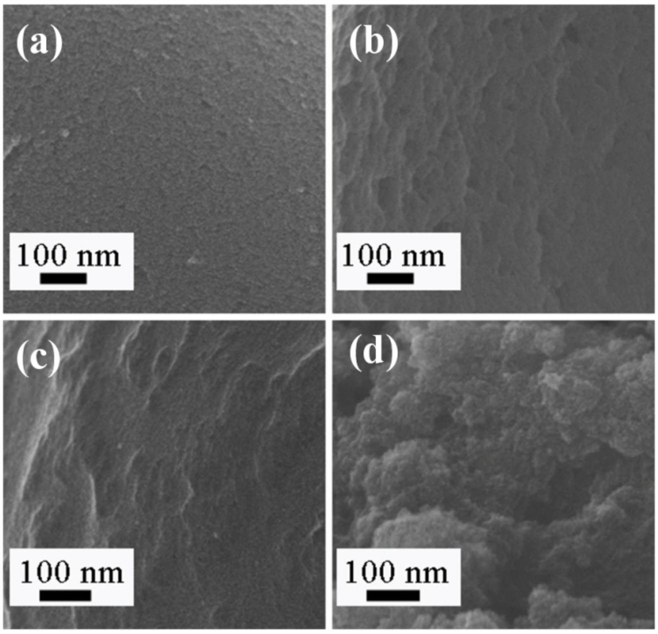


**Fig. S1** High-magnification SEM images of (a) HPC-0.25, (b) HPC-0.5, (c) HPC-1.0 and (d) HPC-1.5.

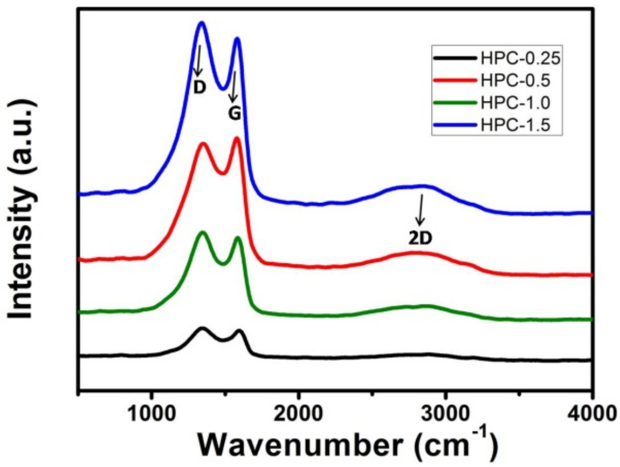


**Fig. S2** Raman spectra of HPC-0.25/-0.5/-1.0/-1.5.

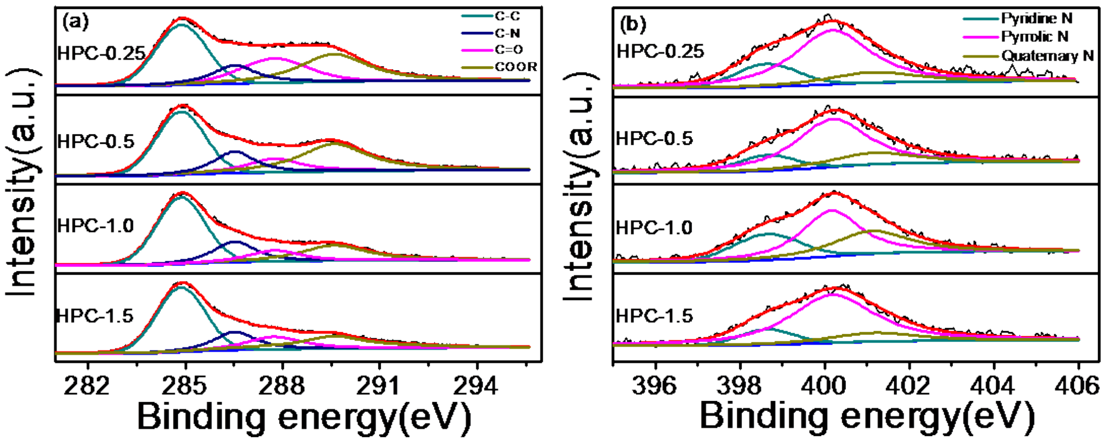


**Fig. S3** (a) C1s and (b) N1s XPS spectra of HPC-0.25/-0.5/-1.0/-1.5.

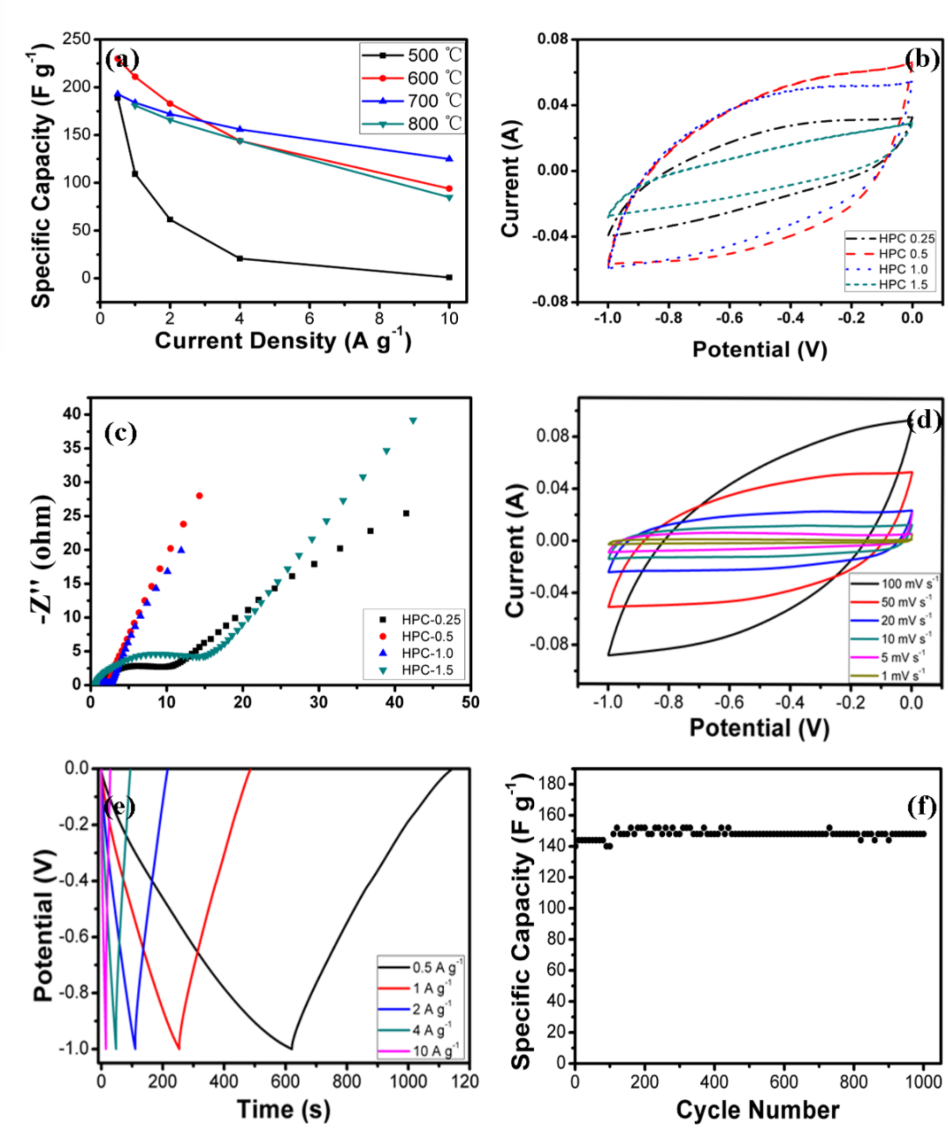


**Fig. S4** Electrochemical performances of the HPCs in 6 mol $L^{-1}$ KOH: (a) specific capacitance of HPC-0.25 prepared at different temperatures, (b) CV curves of HPC-0.25/-0.5/-1.0/-1.5 at a scan rate of 50 mV $s^{-1}$, (c) EIS curves of HPC-0.25/-0.5/-1.0/-1.5, (d) CV curves of HPC-0.5 at different scan rates, (e) GCD curves of HPC-0.5 at different current densities, (f) cycling stability of HPC-0.5 at a current density of 10 A $g^{-1}$.

The CV, GCD and EIS measurements were performed in a three-electrode system at room temperature in 6.0 mol $L^{-1}$ KOH aqueous solution using a CHI 660D electrochemical station. The tested electrodes were prepared according to Ref.1. The mass of loaded active materials is 5 mg.

Firstly, the capacitance of HPCs with the same ratio (0.25) of KOH to EDTA annealed at different temperatures (500, 600, 700, and 800 ℃, denoted as HPC-500, HPC-600, HPC-700, and HPC-800, respectively) were measured with applied voltage from 0 to 1.0 V. As shown in Fig. S4a, these materials had the similar specific capacitances of ~ 190 F $g^{-1}$ at a current density of 0.5 A $g^{-1}$ except for the sample annealed at 500 ℃. Moreover, the capacitance of HPC-500 faded quickly as current density increased, which we attributed to the poor conductivity of the electrode material. HPC-700 showed slightly lower specific capacity at 0.5 A $g^{-1}$ but much higher rate capability while HPC-600 output even higher specific capacity at lower current density, indicating better conductivity and less functionality benefited a lot to comprehensive performance. After balancing input energy and overall performance, we chose 600 ℃ as the optimal annealing temperature.

Alkaline CV behaviors of the samples HPC-0.25/-0.5/1.0/1.5 were first collected at the scanning rate of 50 mV $s^{-1}$ and depicted in Fig. S4b. As presented, rectangular CV curves indicated the mechanism of double electrode layer formation. Compared to the others, the largest voltammogram area of HPC-0.5 could be simply translated into the highest capacitance. Further evidence was given in Fig. S4c that HPC-0.5 showed the lowest ohmic resistance, suggesting a facilitated electronic/ionic transfer. Detailed CV curves (at different scan rates of 1, 5, 10, 20, 50, and 100 mV $s^{-1}$) and GCD (at different current densities of 0.5, 1, 2, 4 and 10 A $g^{-1}$) of HPC-0.5 were showed in Fig. S4d and S4e, respectively. Near rectangular CV and linear GCD profiles were suggesting a superior capacitance behavior. Estimated from the GCD curves, HPC-0.5 showed a high capacitance of 260 F $g^{-1}$ at 0.5 A $g^{-1}$ and 235 F $g^{-1}$ at 1 A $g^{-1}$. The capacitance still retained 148 F $g^{-1}$ at 10 A $g^{-1}$, showing a very good rate capability. The cycling stability of HPC-0.5 at a constant current density of 10 A $g^{-1}$ were measured and shown in Fig. S4f. It displayed a remarkably stable capacitance, without any degradation even after 1000 cycles.

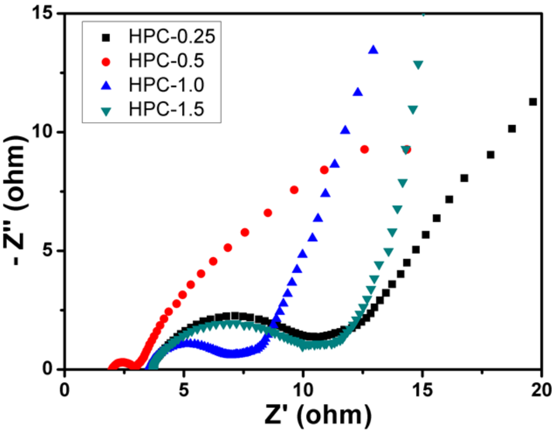


**Fig. S5** EIS measurements of HPC-0.25/ -0.5/ -1.0/ -1.5 in 1 mol $L^{-1}$ NaCl.

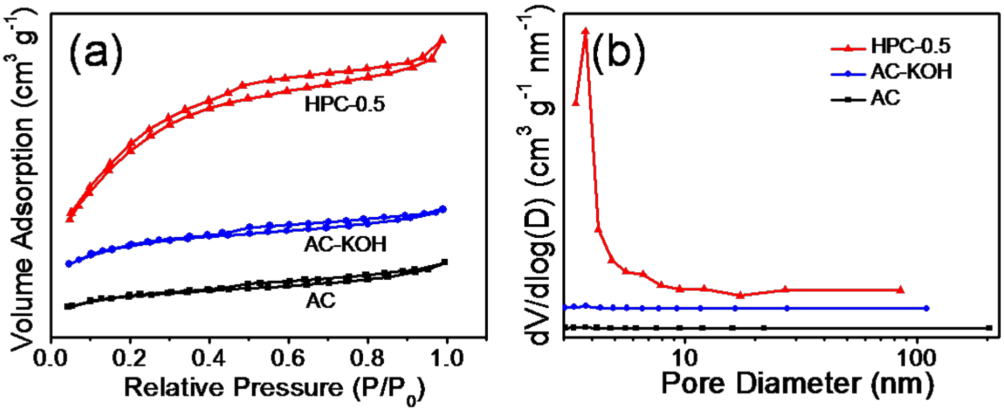


**Fig. S6** (a) $N_2$ adsorption–desorption isotherms and (b) pore size distributions of AC, AC-KOH and HPC-0.5.

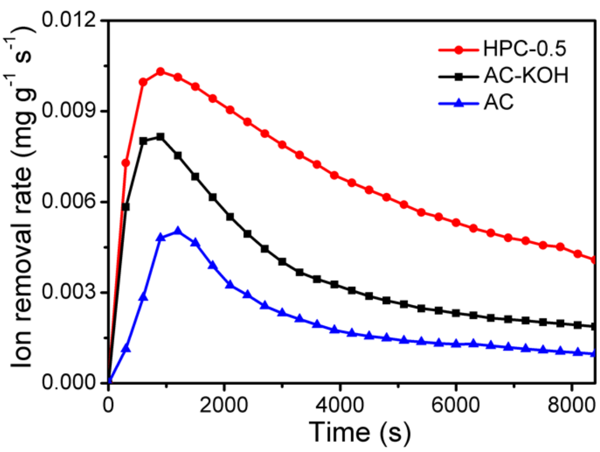


**Fig. S7** Ion removal rates of HPC-0.5, AC and AC-KOH in 40 mg $L^{-1}$ NaCl.

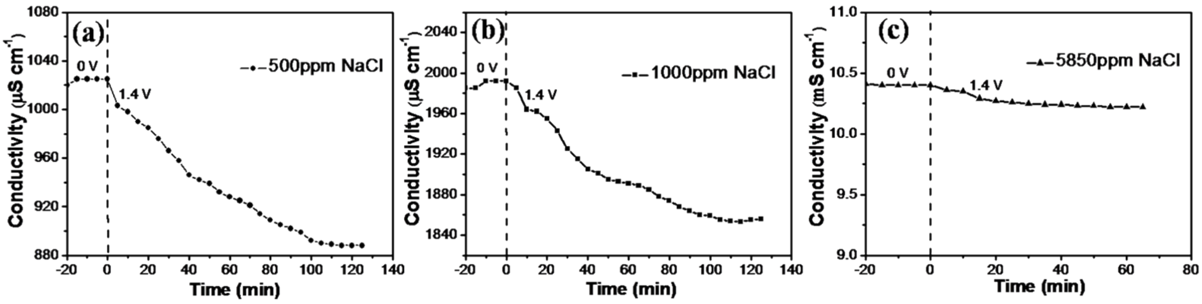


**Fig. S8** The conductivity transients of HPC-0.5 in different concentrations of NaCl.

**Table S1.** Structural data of AC and AC-KOH.

| Sample | $S_{BET}$ $m^2\ g^{-1}$ | $D_{me}$ nm | $V_{total}$ $cm^3\ g^{-1}$ |
|---|---|---|---|
| AC | 779.02 | 2.65 | 0.517 |
| AC-KOH | 869.63 | 2.60 | 0.565 |

**Table S2.** Elemental data of some ions.[2]

| ion | Mass (aum) | Charge | Hydrated radius (nm) | Charge/Radius (a.u.) |
|---|---|---|---|---|
| $Li^+$ | 6.941 | +1 | 0.382 | 2.62 |
| $K^+$ | 39.10 | +1 | 0.331 | 3.02 |
| $Rb^+$ | 85.47 | +1 | 0.329 | 3.04 |
| $Mg^{2+}$ | 24.31 | +2 | 0.428 | 4.67 |
| $Al^{3+}$ | 26.98 | +3 | 0.475 | 6.32 |

1 Y. Fang, B. Luo, Y. Jia, X. Li, B. Wang, Q. Song, F. Kang and L. Zhi, *Adv. Mater.*, 2012, **24**, 6348-6355.
2 J. E. R. Nightingale, *The Journal of Physical Chemistry Letters*, 1959, **63**, 1381-1387.